3D Lagrangian Segmentation with Simultaneous Mesh Adjustment

Karol Mikula and Mariana Remešíková

Abstract We present a method for 3D image segmentation based on the Lagrangian approach. The segmentation model is a 3D analogue of the geodesic active contour model [1] and it contains an additional tangential movement term that allows us to control the quality of the mesh during the evolution process. The model is discretized by the finite volume approach. Segmentation of zebrafish cell images is shown to illustrate the performance of the method.

1 Introduction

A large number of existing 3D image segmentation techniques are based on PDE models representing evolution of 2D surfaces in 3D. Most of them use the level set approach due to its favorable properties with respect to possible topological changes. The other alternative is the Lagrangian approach that directly evolves a 2D surface without viewing it as an isosurface of a three-dimensional function. Because of its two-dimensional character, this technique offers a possibility to obtain faster algorithms. However, even if we do not have to deal with any topological changes in the course of the computation, a Lagrangian method can face the problem of mesh deterioration as a discretized surface evolves. Therefore, in order to successfully apply such methods, we need to have at disposal a mechanism for controlling the quality of the surface discretization during the computation.

Our paper presents a Lagrangian method for 3D image segmentation that allows to adjust the mesh quality along with the surface evolution. The segmentation model contains two normal movement components – one is given by the gradient of an image edge detector function and the other one depends on the edge detector itself and

Karol Mikula, Mariana Remešíková
Department of Mathematics and Descriptive Geometry, Faculty of Civil Engineering, Slovak University of Technology, Radlinského 11, 81368 Bratislava, Slovakia, e-mail: mikula@math.sk, remesikova@math.sk

the mean curvature of the evolving surface. An additional tangential velocity term is added in order to be able to redistribute the mesh points during the evolution. The corresponding PDE is discretized by a finite volume technique and the redistribution is designed so that all control volumes have the same area for $t \to \infty$. The performance of the method is illustrated by examples using microscope images of zebrafish cells.

2 The segmentation model

Let $I\colon \mathbb{R}^3 \supset \Omega \to \mathbb{R}$ be an image intensity function. There are several possibilities how to detect the edges in the image; one of them is to use the edge detector function $e\colon \Omega \to \mathbb{R}$ of the form

$$e(x,y,z) = \frac{1}{1+K\|\nabla I(x,y,z)\|^2} \tag{1}$$

where K is a positive real constant.

Now let X be a two-dimensional Riemannian sphere with metric g_X and $F\colon X \to \Omega \times \langle 0,t_s\rangle$ its time-dependent embedding in Ω. The image of $F^t = F(\cdot,t)$ will be denoted by S^t. The surface S^0 will represent the initial estimate of the surface of the segmented object and S^{t_s} will be the result of the segmentation procedure that should be as close to the actual surface of the segmented object as possible. We let F evolve by the 3D analogue of the geodesic active contour model [1],

$$\partial_t F = a\,(\nabla e \cdot N)\,N + be\Delta_{g_F} F \tag{2}$$

where N is a unit normal to S and $\Delta_{g_F} F$ denotes the Laplace-Beltrami operator with respect to the metric g_F induced on X by F. It is known that $\Delta_{g_F} F$ is equal to the mean curvature vector of F. As we can see from (1), the curvature term is dominant in regions with low intensity changes where e is close to 1 and its gradient is close to 0. On the contrary, the gradient of e becomes significant near the edges where e decreases and approaches 0 for large values of K and $\|\nabla I(x,y,z)\|$. The parameters $a \in \mathbb{R}_+$, $b \in \mathbb{R}_+$ are added to control the influence of the two terms on the segmentation process.

In order to be able to redistribute the mesh points along the surface during the evolution, we enrich (2) with a tangential velocity term. The new model reads

$$\partial_t F = a\,(\nabla e \cdot N)\,N + be\Delta_{g_F} F + v_T = v_N + v_T \tag{3}$$

where v_T is a tangential vector field on S and v_N denotes the normal component of the evolution, $v_N = a\,(\nabla e \cdot N)\,N + be\Delta_{g_F} F$.

In our case, we use an area-oriented tangential redistribution [6] derived from the evolution of the induced metric g_F. Both metrics g_X and g_F induce measures on X; let us denote them by μ_X and μ_F. The Radon-Nikodým derivative $G = \frac{\partial \mu_F}{\partial \mu_X}$ is called

the *area density* of F. It evolves along with F as [3]

$$\partial_t G = (v_N \cdot h + \operatorname{div}_{g_F} w_T)\, G \tag{4}$$

where h is the mean curvature vector of F, w_T is a vector field on X obtained as the pull-back of v_T along F and div_{g_F} denotes the divergence with respect to the metric g_F. From this follows the evolution of the area of S,

$$\partial_t A = \int_X (v_N \cdot h + \operatorname{div}_{g_F} w_T)\, \mathrm{d}\mu_F = \int_X v_N \cdot h \, \mathrm{d}\mu_F. \tag{5}$$

The embedding F^t is called *area uniform with respect to* g_X if its area density G^t is constant. Our redistribution method is based on the requirement $G^t \longrightarrow_{t\to\infty} C$ that is equivalent to the practically more convenient dimensionless condition

$$\frac{G^t}{A^t} \underset{t\to\infty}{\longrightarrow} C.$$

This can be achieved, for example, if $\frac{G}{A}$ satisfies

$$\partial_t \left(\frac{G}{A}\right) = \omega \left(C - \frac{G}{A}\right) \tag{6}$$

where $\omega \in \mathbb{R}_+ \times \langle 0, t_s \rangle$ represents the redistribution speed. Since we know how both G and A evolve, the combination of (4) and (5) with (6) implies that w_T has to satisfy

$$\operatorname{div}_{g_F} w_T = v_N \cdot h - \frac{1}{A} \int_X v_N \cdot h \, \mathrm{d}\mu_F + \omega \left(C \frac{A}{G} - 1\right). \tag{7}$$

Since this condition does not uniquely determine w_T, we suppose, in addition, that w_T is a gradient field, that means $w_T = \nabla_{g_F} \psi$, $\psi \colon X \times \langle 0, t_s \rangle \to \mathbb{R}$. Thus we obtain

$$\Delta_{g_F} \psi = v_N \cdot h - \frac{1}{A} \int_X v_N \cdot h \, \mathrm{d}\mu_F + \omega \left(C \frac{A}{G} - 1\right) \tag{8}$$

that yields a unique solution if we prescribe the value of ψ in one point of X.

3 Numerical approximation of the segmentation model

The time discretization of our segmentation model (3) is semi-implicit,

$$\frac{F^n - F^{n-1}}{\tau} = a \left(\nabla e \cdot N^{n-1}\right) N^{n-1} + be \Delta_{g_{F^{n-1}}} F^n + v_T^{n-1}. \tag{9}$$

The space discretization is based on the finite volume approach and it includes two meshes – the mesh discretizing the surface S^n and the voxel grid of the image

used to approximate e and ∇e. First, let us consider a triangulation of X which is a simplicial complex homeomorphic to X. The corresponding homeomorphism induces a triangular structure on X consisting of vertices X_i, $i = 1 \dots n_v$, edges e_j, $j = 1 \dots n_e$, and triangles $\mathscr{T}_k$, $k = 1 \dots n_t$.

Now we construct the control volume mesh (Figure 1). The point X_i is the common vertex of m mesh triangles $\mathscr{T}_1, \dots, \mathscr{T}_m$ and m edges $e_1, \dots, e_m$, where e_p connects X_i with its neighbor X_{i_p} (we use local indexing for simplicity). The triangle $\mathscr{T}_p$ admits a barycentric coordinate system – each point of the triangle can be expressed as $P = \lambda_1 X_i + \lambda_2 X_{i_p} + \lambda_3 X_{i_{p+1}}$ where $\lambda_1 + \lambda_2 + \lambda_3 = 1$. Let B_p be the barycenter of $\mathscr{T}_p$ and C_p the center of e_p, $p = 1 \dots m$, and let the barycentric subdivision of $\mathscr{T}_p$ be constructed using these points. The control volume V_i corresponding to X_i is constructed as the union of the triangles $\mathscr{V}_{p,1} = M_i C_p B_p$ and $\mathscr{V}_{p,2} = M_i B_p C_{p+1}$ for $p = 1 \dots m$ where we set $C_{m+1} = C_1$. Each triangle contains two control volume edges $\sigma_{p,1} = C_p B_p$, $\sigma_{p,2} = B_p C_{p+1}$.

The manifold X can be embedded in $\mathbb{R}^3$ by $\bar{F}^n$, a piecewise linear approximation of F^n. First, we set $\bar{F}^n(X_i) = F^n(X_i)$. Then, for any triangle $\mathscr{T}_p$ with vertices X_i, X_{i_p}, $X_{i_{p+1}}$, we set $\bar{F}^n(\lambda_1 X_i + \lambda_2 X_{i_p} + \lambda_3 X_{i_{p+1}}) = \lambda_1 F^n(X_i) + \lambda_2 F^n(X_{i_p}) + \lambda_3 F^n(X_{i_{p+1}})$. The embedding $\bar{F}^n$ induces a metric g^n on X which induces a measure μ^n on X.

The surface $\bar{S}^n = \bar{F}^n(X)$ is a polyhedron with vertices $\bar{F}^n(X_i) = F^n(X_i) = F_i^n$, edges $\bar{e}_j^n = \bar{F}^n(e_j)$ and triangular faces $\bar{\mathscr{T}}_p^n = \bar{F}^n(\mathscr{T}_p)$. The approximation of the unit normal to S^n at F_i^n is denoted by N_i^n. We will use the notation $\nu_{p,1}^n$, $\nu_{p,2}^n$ for the outward unit normals to $\bar{F}^n(\sigma_{p,1})$ and $\bar{F}^n(\sigma_{p,2})$ in the plane of $\bar{\mathscr{T}}_p^n$. Further, $\theta_{p,1}^n$ and $\theta_{p,2}^n$ will represent the angles of $\mathscr{T}_p$ adjacent to X_{i_p} and $X_{i_{p+1}}$, respectively, measured in the metric g^n.

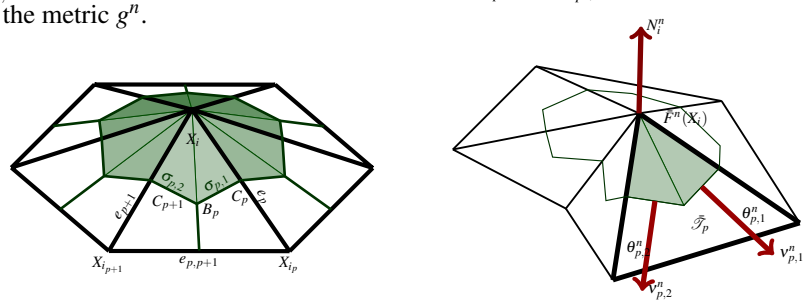

Fig. 1 The surface discretization mesh. Left, the triangulation of the topological sphere X. Right, the corresponding approximation of the embedded surface $F^n(X)$.

Integrating (9) over V_i, we obtain

$$\int_{V_i} \frac{F^n - F^{n-1}}{\tau} \, \mathrm{d}\mu_{F^{n-1}} = \int_{V_i} a \left(\nabla e \cdot N^{n-1} \right) N^{n-1} \, \mathrm{d}\mu_{F^{n-1}} + \int_{V_i} be \Delta_{g_{F^{n-1}}} F^n \, \mathrm{d}\mu_{F^{n-1}} + \int_{V_i} v_T^{n-1} \, \mathrm{d}\mu_{F^{n-1}}. \tag{10}$$

The term on the left hand side can be approximated simply by

$$\int_{V_i} \frac{F^n - F^{n-1}}{\tau} \, \mathrm{d}\mu_{F^{n-1}} \approx \mu^n(V_i) \frac{F_i^n - F_i^{n-1}}{\tau}. \tag{11}$$

In order to approximate $\|\nabla I\|$, e and ∇e, we use the voxel structure of the image I. Let us suppose that the voxels are cubes with side length h. The voxel with coordinates $x \in \mathbb{N}$, $y \in \mathbb{N}$, $z \in \mathbb{N}$ will be denoted by P_j, $j = (x,y,z)$. Since X is embedded in the image domain Ω, the voxel coordinates corresponding to F_i^n are obtained simply by rounding its coordinates. The representative value of I and e in P_j will be denoted by I_j and e_j. Further, v_1, v_2 and v_3 are the standard basis vectors in $\mathbb{R}^3$. The 6 voxel faces will be represented by $F_j^{\pm p}$, $p = 1,2,3$.

First, let us construct the approximation of ∇I in the barycenter $c_j^{\pm p}$ of $F_j^{\pm p}$. The derivative in the direction of v_p is discretized by

$$D^{\pm p} I_j = \pm \left(I_{j \pm v_p} - I_j \right) / h.$$

For the other two directions v_q, $q \neq p$, we will use the values of I in the centers of the voxel edges $F_j^{\pm p, \pm q}$; we denote them by $I_{j \pm \frac{1}{2} v_p \pm \frac{1}{2} v_q}$. Then we use

$$D^{\pm p,q} I_j = \frac{I_{j \pm \frac{1}{2} v_p + \frac{1}{2} v_q} - I_{j \pm \frac{1}{2} v_p - \frac{1}{2} v_q}}{h}, \quad I_{j \pm \frac{1}{2} v_p \pm \frac{1}{2} v_q} = \frac{I_j + I_{j \pm v_p} + I_{j \pm v_q} + I_{j \pm v_p \pm v_q}}{4}.$$

Finally, we take

$$Q_j^{\pm p} = \left((D^{\pm p} I_j)^2 + \sum_{p \neq q} (D^{\pm p,q} I_j)^2 \right), \quad \|\nabla I(x,y,z)\|^2 \approx \left(\sum_{p=1}^{3} (Q_j^{+p} + Q_j^{-p}) \right) / 6. \tag{12}$$

The gradient of e is computed analogously.

Now, the surface normal at F_i^n is approximated by the arithmetic mean of the normals to all triangles containing F_i^n. This completes the approximation of the first term on the right hand side of (10). As for the second term, we use

$$\int_{V_i} b e \Delta_{g_{F^{n-1}}} F^n \, \mathrm{d}\mu_{F^{n-1}} \approx b_i e_i \frac{1}{2} \sum_{p=1}^{m} \left(\cot \theta_{i,p-1,1}^{n-1} + \cot \theta_{i,p,2}^{n-1} \right) (F_i^n - F_{i_p}^n) \tag{13}$$

where we used the cotangent scheme [4] to discretize the Laplace-Beltrami operator. The value e_i is the value of e in the voxel containing F_i^n. We consider $\theta_{i,0,1}^{n-1} = \theta_{i,m,1}^{n-1}$.

The last term to discretize is the integral of the tangential velocity. Since w_T^n is a gradient field, the following version of the Stokes theorem applies [2, 6]

$$\int_{V_i} v_T^{n-1} \, \mathrm{d}\mu_{F^{n-1}} = \int_{\partial V_i} \psi^{n-1} \nu_i^{n-1} \, \mathrm{d}H_{\mu_{F^{n-1}}} - \int_{V_i} \psi^{n-1} h^{n-1} \, \mathrm{d}\mu_{F^{n-1}}.$$

This yields the approximation

$$\int_{V_i} v_T^{n-1}\,\mathrm{d}\mu_{F^{n-1}} \approx \sum_{p=1}^{m}\left(\|\sigma_{i,p,1}\|_{n-1}\psi_{i,p,1}^{n-1}v_{i,p,1}^{n-1} + \|\sigma_{i,p,2}\|_{n-1}\psi_{i,p,2}^{n-1}v_{i,p,2}^{n-1}\right) - \mu^{n-1}(V_i)\psi_i^{n-1}h_i^{n-1} \tag{14}$$

where $\|\cdot\|_{n-1}$ denotes the length computed by the metric g^{n-1} and $\psi_{i,p,1}^{n-1}$, $\psi_{i,p,2}^{n-1}$ are the values of ψ^{n-1} in the midpoints of $\sigma_{i,p,1}$ and $\sigma_{i,p,2}$. They are obtained from the values of ψ^{n-1} in the vertices X_i by linear interpolation.

The function ψ is computed from (8) where, again, we use the cotangent scheme to discretize the Laplace-Beltrami operator of ψ^{n-1}. This scheme is also used to approximate the mean curvature vector h, namely

$$h_i^{n-1} = \frac{1}{\mu^{n-1}(V_i)}\sum_{p=1}^{m}\left(\cot\theta_{i,p-1,1}^{n-1} + \cot\theta_{i,p,2}^{n-1}\right)(F_i^n - F_{i_p}^n). \tag{15}$$

The area of S^{n-1} is approximated by

$$A^{n-1} = \sum_{i=1}^{n_v}\mu^{n-1}(V_i). \tag{16}$$

Alternatively, $A(t^{n-1})$ could be approximated as

$$A(t^{n-1}) = \int_X G(x,t^{n-1})\,\mathrm{d}\mu_X \approx \sum_{i=1}^{n_v} G_i^{n-1}\mu_X(V_i).$$

This leads to an approximation of the volume density G^{n-1}. Since we did not particularly specify μ_X, we can assume that $\mu_X(X) = 1/C$ and $\mu_X(V_i) = \mu_X(X)/n_v$ for all $i = 1\ldots n_v$. Then we can set

$$G_i^{n-1} = \mu^{n-1}(V_i)\frac{n_v}{\mu_X(X)} = Cn_v\mu^{n-1}(V_i), \qquad C\frac{A}{G} \approx \frac{A^{n-1}}{n_v\mu^{n-1}(V_i)}. \tag{17}$$

4 Experiments

Finally, we present two examples of segmentation of biological images. The images display cell nuclei and cell membranes of a zebrafish embryo. Segmentation of cell nuclei and cells has a large number of applications [5]. Particularly, segmentation in form of a triangulated surface can be easily used to compute the area of the surface of a cell or to evaluate the shape of a cell. Before segmenting, the images were pre-filtered by the geodesic mean curvature flow method [1].

In both experiments, we used a relatively large value of ω. Since the tangential direction is approximated, for such large values, the points tend to deviate from the surface where they should be situated [6]. In order to overcome this difficulty,

in each time step we first perform the corresponding normal movement, then the tangential movement and afterwards we project the new vertices on the surface obtained by the normal movement alone.

The first experiment deals with the nucleus image. We show segmentation of a single cell nucleus. We performed 400 time steps and the model parameters were set to $n_v = 258$, $\tau = 0.001$, $h = 1.0$, $\omega = 100.0$, $a = 1.0$, $b = 200.0$ for time steps $1 \ldots 200$ and $b = 1.0$ after. The initial condition was a sphere centered in a manually estimated nucleus center. Figure 2 shows two different 2D slices of the data, the initial surface and the segmentation result. Figure 3 shows the effect of the tangential redistribution of mesh points during the computation. We can see that the tangential movement leads to more evenly distributed mesh points and thus a more correct representation of the surface. Quantitatively evaluated, the ratio of the minimal and maximal control volume area was 0.176 when no redistribution was applied while it reached 0.894 when the redistribution step was included.

In the second experiment, we segmented several cells from the membrane image. Membrane data are usually of a worse quality and more difficult to segment than nucleus data. We performed 400 time steps and we used $n_v = 258$, $\tau = 0.003$, $h = 1.0$, $\omega = 100.0$, $a = 3.0$, $b = 20.0$ for time steps $1 \ldots 200$ and $b = 1.0$ after. Similarly to the case of nucleus segmentation, the initial surface was a sphere (of the same radius for all cells). Figure 4 shows a 2D slice of the image, the initial surfaces and the segmented cells. Figure 5 shows the whole segmented cells.

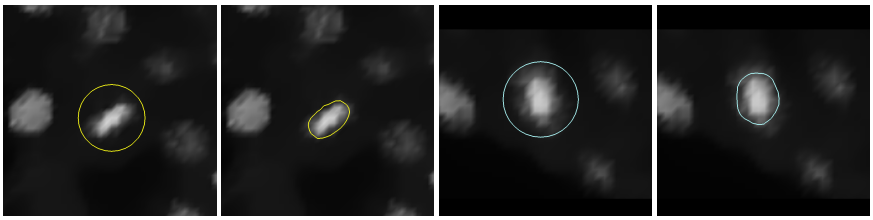

Fig. 2 Cell nucleus segmentation – the data, the initial surface and the segmented surface shown in two different 2D slices.

Acknowledgement

This work was supported by the grants APVV-0184-10 and VEGA 1/1137/12.

References

1. Caselles, V., Kimmel, R., Sapiro, G.: Geodesic active contours. International Journal of Computer Vision **22**, 61–79 (1997)
2. Dziuk, G., Elliott, C.: Finite elements on evolving surfaces. IMA J. Numer. Anal. **27**, 262–292 (2007)

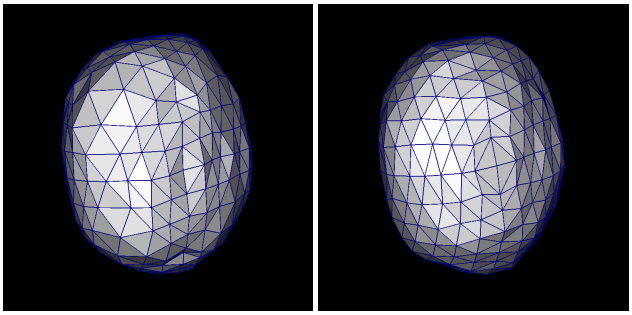

Fig. 3 Cell nucleus segmentation. Left, the segmented nucleus surface obtained with no tangential redistribution. Right, the surface obtained with tangential redistribution of mesh points, $\omega = 100.0$.

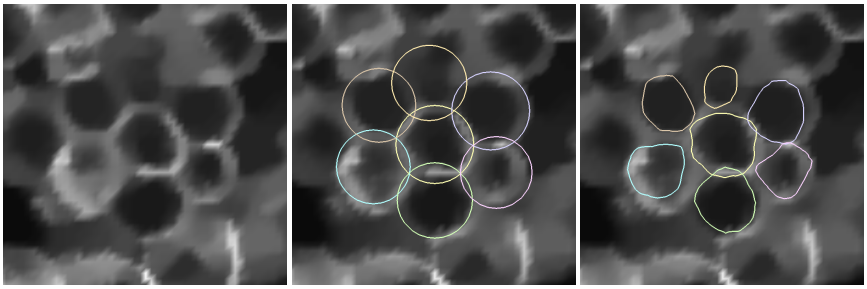

Fig. 4 Cell membrane image segmentation – 2D slices of the data, of the initial condition and of the segmented surfaces.

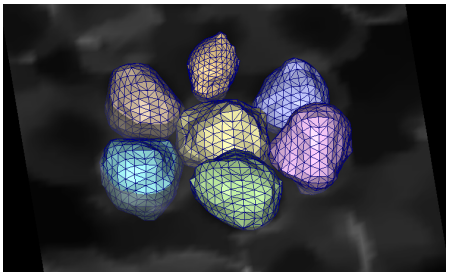

Fig. 5 Cell membrane image segmentation – the segmented surfaces.

3. Mantegazza, C.: Lecture notes on mean curvature flow. Springer (2011)
4. Meyer, M., Desbrun, M., Schroeder, P., Barr, A.: Discrete differential geometry operators for triangulated 2manifolds. Visualization and Mathematics **III**, 35–57 (2003)
5. Mikula, K., Peyrieras, N., Remesikova, M., Stasova, O.: Segmentation of 3d cell membrane images by pde methods and its applications. Computers in Biology and Medicine **41**(6), 326–339 (2011)
6. Mikula, K., Remesikova, M., Sarkoci, P., Sevcovic, D.: Surface evolution with tangential redistribution of points. submitted (2013)